Hydrothermal synthesis, thermal decomposition and optical properties of Fe2F5(H2O)(Htaz)(taz)(Hdma)

Mouna Smida, Jérôme Lhoste, Mohamed Dammak, Santiago García-Granda

Arabian Journal of Chemistry (2019) **12**, 2519–2523

King Saud University

Arabian Journal of Chemistry

www.ksu.edu.sa
www.sciencedirect.com

ORIGINAL ARTICLE

Hydrothermal synthesis, thermal decomposition and optical properties of $Fe_2F_5(H_2O)(Htaz)(taz)(Hdma)$

Mouna Smida [a,*], **Jérome Lhôste** [c], **Mohamed Dammak** [a], **Santiago Garcia-Granda** [b]

[a] *Laboratoire de Chimie Inorganique, Faculté des Sciences de Sfax, Université de Sfax, BP 1171, Sfax 3000, Tunisia*
[b] *Département de Chimie Physique Analytique et Chimie Organique et Inorganique, Université d'Oviedo, CINN, 33006 Oviedo, Spain*
[c] *IMMM-UMR 6283 CNRS, LUNAM, Faculté des Sciences et Techniques, Université du Maine, Avenue Olivier Messiaen, 72085 Le Mans Cedex 9, France*

Received 16 June 2014; accepted 19 April 2015
Available online 25 April 2015

KEYWORDS

Thermal analysis;
Mass spectrometry;
UV–vis

Abstract Crystal structure of $Fe_2F_5(H_2O)(Htaz)(taz)(Hdma)$ which crystallizes in the triclinic system space group $P\bar{1}$ with unit cell parameters $a = 8.8392(5)$ Å, $b = 9.1948(5)$ Å, $c = 9.5877(5)$ Å, $\alpha = 82.070(3)°$, $\beta = 63.699(3)°$, $\gamma = 89.202(3)°$, $Z = 2$, and $V = 690.91(7)$ Å^3, was synthesized under hydrothermal conditions at 393 K for 72 h, by a mixture of FeF_2/FeF_3, 1,2,4-triazole molecule (Htaz), and hydrofluoric acid solution (HF 4%) in dimethylformamide solvent (DMF). The main feature of this material is the coexistence of two oxidation states for iron atoms (Fe^{2+}, Fe^{3+}) in the unit cell, which associate by opposite fluorine corners of FeF_5N and FeF_2N_4 octahedra, and/or triazole molecule which originates the 2D produces material. The structure determination, performed from single crystal X-ray diffraction data, lead to the $R_1/_wR_2$ reliability factors 0.031/0.087. Thermal stability studies (TG/DTG/DTA) show that the decomposition provides in the temperature range 473–773 K and no mass loss was detected before 473 K. Mass spectrometry (MS) has been used. The optical absorption of the solid was measured at the corresponding λ_{max} using UV–vis diffuse-reflectance spectrum.

1. Introduction

New hybrid fluoride materials in which the dimensionality of the metal fluoride entities is isolated polyanions or clusters 0D (Adil et al., 2009), infinite chains 1D (Goreshnik et al., 2002), layers 2D (Adil et al., 2010), and 3D cavities with different cations such as Zn, Mn, Al and Fe (Lin et al., 2009; Pachfule et al., 2010; Cadiau et al., 2011; Smida et al., 2013),

* Corresponding author. Tel.: +216 95 231 854/+216 28 742 375.
E-mail address: mouna.smida@yahoo.fr (M. Smida).
Peer review under responsibility of King Saud University.

Production and hosting by Elsevier

http://dx.doi.org/10.1016/j.arabjc.2015.04.023
1878-5352

are being investigated. A series of isolated polyhedral containing the transition metal fluorides is reported in the literature, such as FeF_6 (Adil et al., 2006), $FeF_2(H_2O)_4$ (Ben Ali et al., 2009), FeF_5H_2O (Malinovskii et al., 2008), and $FeF_3(H_20)_3$ (Adil et al., 2007). Thus Kiriasis and Mattes (1991) and Bentrup et al. (1991) showed two compounds built up dimmers of iron fluoride are Fe_2F_9 and $Fe_2F_8(H_2O)_2$. The infinite chains exhibiting FeF_6 and $Fe_2(H_2O)_4F_6$ were respectively reported by Herdtweck et al. (1990), Frommen et al. (1995) and Smida et al. (2013). Few framework structures are reported except for the two new structures built from $Fe_2F_5(taz)_2$ and as far as we know $Fe_2F_5(H_2O)(Htaz)(taz)$ layers; and only a 3D hybrid fluoroferrate has been evidenced (Smida et al., 2013).

Most often, the metal fluoride compounds, which result from the condensation of MX_n units (X = F, O, N), are few materials that exhibit extended 2D layers with open structure, such as $[Cu(C_{10}H_8N_2)_2(H_2O)_2][MoO_2F_4]$ and $[Cu(C_{10}H_8N_2)_2(H_2O)_2][NbOF_5]$ with Cu, Mo and Nb octahedral coordinated (Mahenthirarajah et al., 2009).

It is commonly accepted that the shape and size of amine cations play a significant role on the formation of organically templated microporous solids. The formation of hybrid compounds microporous containing transition metal fluorides, organic entities, and with more than one ligand, is very scarce and the experimental synthetic conditions play a fundamental role, such as the molar ratio of reagents, nature of structure directing agents, pH, solvents, temperature and time of reaction (Liu et al., 2009; Su et al., 2010). These materials are prepared under solvothermal conditions, by reactions between the inorganic and organic parts lead up to two types of hybrid networks (Sanchez and Ribot, 1994). The first type or Class I hybrid fluorides, where the metal atoms and organic compounds are associated by weak interactions such as Van der Waals or Hydrogen bonds, while for the second type, Class II hybrid network, the connection is ensured by strong covalent or iono-covalent bonds such as in the $Fe_2F_5(H_2O)(Htaz)(taz)(Hdma)$ structure.

Extensive research interests have in recent years been attracted to the construction and exploration of porous metal–organic frameworks or MOF'S (Férey, 2007) which built up from transition metal fluorides and organic molecules for applications in areas such as gas selective adsorption (especially hydrogen) (Collins and Zhou, 2007), ion exchange (Halper et al., 2006), catalysis (Zou et al., 2006) and batteries preparation (Férey et al., 2007). In the application of them to the preparation of batteries, Li-ion batteries represent the most advanced battery technology with the highest specific energy among all the rechargeable batteries currently commercialized (Férey et al., 2007). In this paper we describe and discuss the results of our investigation about a new hybrid iron fluoride, which has been determined by X-ray diffraction, and characterized by thermogravimetric analysis (TG/DTG), mass spectrometry (m/z 15, m/z 44) and UV–vis spectroscopy.

2. Experimental section

The compound is prepared in hydrothermal conditions at 393 K under autogenous pressure using classical heating (Parr Autoclave) for 72 h, afterwards cooled to room temperature. The starting materials were the following: FeF_2/FeF_3; hydrofluoric acid solution (40% HF, Riedel-de Haen), 1,2,4-triazole (Htaz) and dimethylformamide DMF solvent (99.8%, Sigma Aldrich), filling 50% of the Autoclave Parr. The solid products were washed with DMF and dried at room temperature. The results showed a new mixed hybrid fluoride, where crystals appeared in brown colour. X-ray crystal data were collected at room temperature on APEX II Quazar (4-circle Kappa goniometre, IμS microfocus source Mo Kα) such that single crystal was carefully selected under a polarizing microscope. The structure was solved by direct methods using **SHELXS-86** which give the positions of most of the atoms (iron, nitrogen, fluorine atoms), and extended by Fourier maps **SHELXL-97** (Sheldrick, 1986, 1997), included in **WINGX** package (Farrugia, 1999). The structure graphics were created by the **DIAMOND** program (Brandenburg and Berndt, 1999). Crystal data and structure refinement details for the title compound are given in Table 1. Scanning Electronic Microscopy showed the morphology of $Fe_2F_5(H_2O)(Htaz)(taz)(Hdma)$ and confirmed that all non-hydrogen atoms are present: Fe, F, O, N and C.A. Mettler-Toledo TGA/SDTA851ELF was used for the thermal analyses in oxygen dynamic atmosphere (50 mL/min) at a heating rate of 10 °C/min. The masses of samples used in TG and DTA measurements were 5.7035 mg. In TG tests, a Pfeiffer Vacuum ThermoStar™ GSD301T mass spectrometer was used to determine the evacuated vapours. The masses 15(NH_3) and 44(CO_2) were tested using a detector C-SEM, operating at 1200 V, with a time constant of 1 s. The UV–vis diffuse-reflectance spectrum was measured at room temperature between 200 and 800 nm (6.2–1.55 eV) using OLIS 14-VIS–NIR spectroscopy operating system. The reflectivity spectra were transformed to absorption

Table 1 Crystallographic data of $Fe_2F_5(H_2O)(Htaz)(taz)(Hdma)$ at room temperature.

Crystal data formula	$Fe_2F_5N_7O\ C_6H_{15}$
Crystal system	Triclinic
Space group	$P\bar{1}$
a (Å)	8.8392(5)
b (Å)	9.1948(5)
c (Å)	9.5877(5)
α (°)	82.070(3)
β (°)	63.699(3)
γ (°)	89.202(3)
V (Å^3)	690.91(7)
Z	2
$F(000)$	406
Formula weight (g mol^{-1})	407.93
Dimensions (mm)	$0.13 \times 0.11 \times 0.05$
μ (mm^{-1})	2.175
ρ calculated (g cm^{-3})	1.951
Temperature (K)	296
θ range (°)	2.24/25.04
Limiting indices	$-10 \leqslant h \leqslant 10$
	$-10 \leqslant k \leqslant 10$
	$-11 \leqslant l \leqslant 11$
Collected reflections	10,958
Reflections unique	2049
Parameter refined	189
Goodness of fit (F^2)	1.194
R_1 [$I > 2\sigma I$]	0.0311
WR_2	0.0875
ρ min/max (e Å^{-3})	−0.84/0.72

(α/S) spectra by the Kubelka–Munk function: $F(R) = \alpha/S = (1 - R)^2/2R$, where R is the reflectivity at a given wavelength, α is the absorption coefficient, and S is the scattering coefficient (Kubelka, 1948; Vargas, 2002). The optical gap value was determined from the intersection of the wavelength axis and the extrapolated line of the linear portion at the absorption threshold.

3. Results and discussion

3.1. Structural study

X-ray single crystal analysis of $Fe_2F_5(H_2O)(Htaz)(taz)(Hdma)$ shows that this compound crystallizes in the triclinic system space group $P\bar{1}$. The structure is built by $Fe_2F_5(H_2O)(Htaz)(taz)$ anionic layers separated by dimethylammonium cations (Hdma). These layers are parallel to the c direction. The coordination sphere around Fe(II) of $FeN_4(H_2O)_2$ octahedra in our compound shows the same atoms and the similar range of distances as for $[Fe(dtm)_2(H_2O)_2(ClO_4)_2{\cdot}2(H_2O)]$ and $[Fe(btx)_3(H_2O)_2(ClO_4)_2(H_2O)_2(btx)]$ compounds, also with similar solid state structure since all crystallize in the triclinic centrosymmetric space group $P\bar{1}$ (Xing et al., 2011; Dong, 2006). In particular the first shows one almost identical unit cell. Fig. 1 shows that the layers are built up from $FeN_4(H_2O)_2$ octahedra and $Fe_3F_{10}N_6$ trimers, which are connected by two neutral and two deprotonated triazole molecules along the $[1\,\bar{1}\,0]$ and $[1\,1\,0]$ directions, respectively. The main feature in this new bidimensional structure $Fe_2F_5(H_2O)(Htaz)(taz)(Hdma)$ is the arrangement of different polyhedral in the unit cell, connected by triazole ligands which make the building of the crystal forming anionic layers where [Hdma] cations are placed. However, the $Fe_3F_{10}N_6$ trimers result of two FeF_5N and one FeF_2N_4 octahedra linked by two fluorine atoms. The $Fe(3)F_2N_4$ octahedra which links with two long Fe(3)—F(1) distances by symmetry (2.046(2) Å), underrating that the oxidation state is +2 for Fe(3) iron atoms (Ben Ali et al., 2009). The Fe(3) iron atoms associated with four nitrogen atoms from triazole molecule were the Fe(3)—N bond length have two values 2.179(3) Å and 2.205(3) Å. It must be noted that the bonds established between Fe(3) and nitrogen atoms allow to deduce that the compound is a Class II hybrid. In fact the F—Fe(3)—F and N—Fe(3)—N angles values are equal to 180°. The $Fe(1)F_5N$ octahedra includes one nitrogen atom of triazole molecule, and the Fe(1)—F distances are between 1.891(2) Å and 1.989(2) Å which proves that the oxidation state is +3 for Fe(1) iron atom. In $Fe^{II}N_4(H_2O)_2$ monomeric octahedral, the Fe(2)—O bond length is 2.187(3) Å, while the O—Fe(2)—O angle is 180°.

3.2. Thermal behaviour

A thermal analysis of $Fe_2F_5(H_2O)(Htaz)(taz)(Hdma)$ compound was performed in the temperature range 298–973 K. The DTG/TG, ATD curves and the mass spectrometric analysis are depicted in Figs. 2 and 3, respectively. The thermogravimetric curve TG reveals that the compound $Fe_2F_5(H_2O)(Htaz)(taz)(Hdma)$ is stable until 473 K and only one mass loss was detected before 773 K. This only step between 473 and 773 K, associated with an exothermic peak on ATD curve, which may be due to the loss of two water molecules weakly bound to iron II, characterized by a distance Fe^{II}—O (2.187 Å), of $Fe^{II}N_4(H_2O)_2$ octahedra, and the degradation of the organic molecules give the FeF_3 at 773 K (Ben Ali et al., 2009). A similar observed curve was described for the parent complexes obtained by FeF_2/FeF_3-taz-HF system in DMF (dimethylformamide) solvent (Smida et al., 2013). The experimental mass loss value is 40% and the residual powder corresponds to haematite compounds. However, the FeF_3 is slightly contaminated to leading to Fe_2O_3 at 923 K (contaminated with a small amount of carbon graphite particles Cg) (Ben Ali et al., 2009). The associated mass spectrometry m/z 15 and m/z 44 curves are confirming the TG/DTG conclusions. We have plotted the main volatiles formed during $Fe_2F_5(H_2O)(Htaz)(taz)(Hdma)$ decomposition. m/z 15 curve has one maxima which coincides with the maxima of m/z 44 curve at the same temperature 705 K. The mass spectrometric (m/z 15) curve is associated with the maximum of m/z 44 curve which are attributed to one slow and continuous step

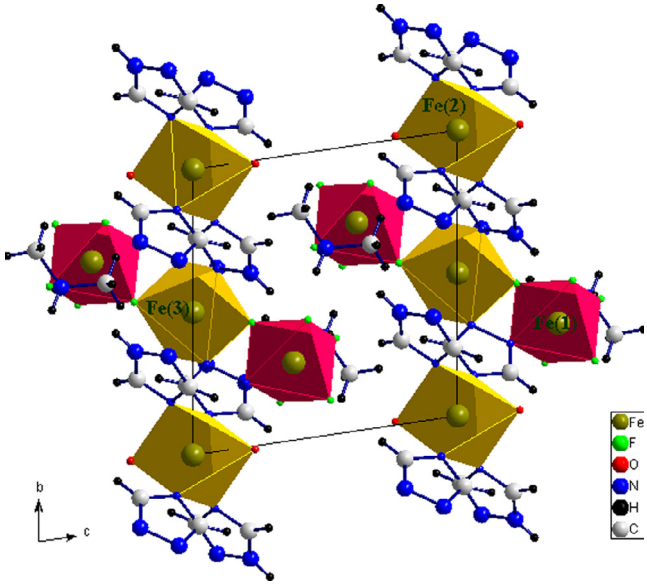

Figure 1 Projection of $Fe_2F_5(H_2O)(Htaz)(taz)(Hdma)$ crystal structure in the (b and c) plane.

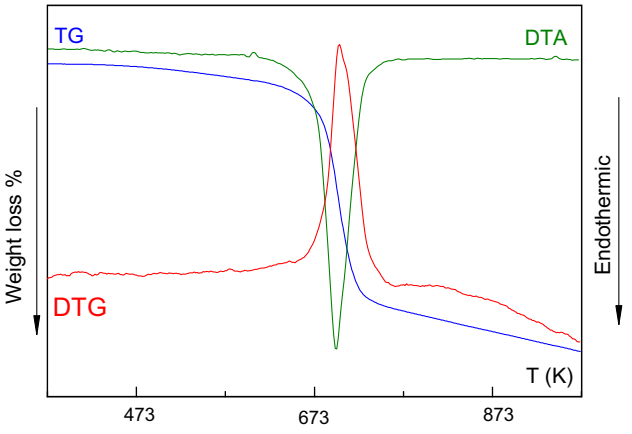

Figure 2 TG–DTG–DTA heating of $Fe_2F_5(H_2O)(Htaz)(taz)$-(Hdma) material.

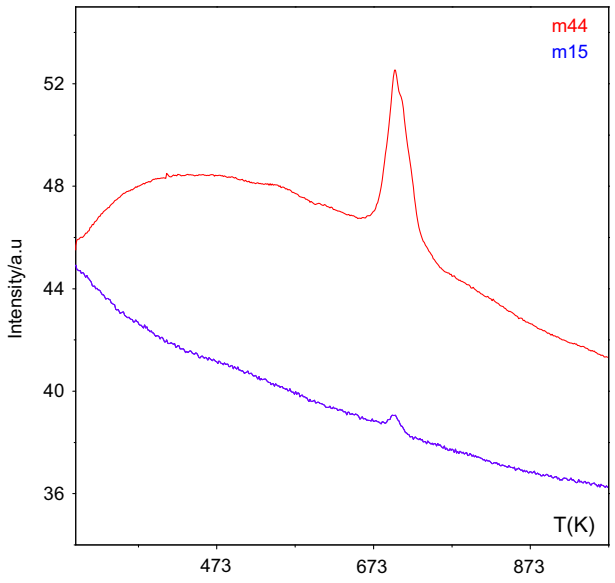

Figure 3 m/z 15(NH_3) and 44(CO_2) MS signals of evacuated vapours.

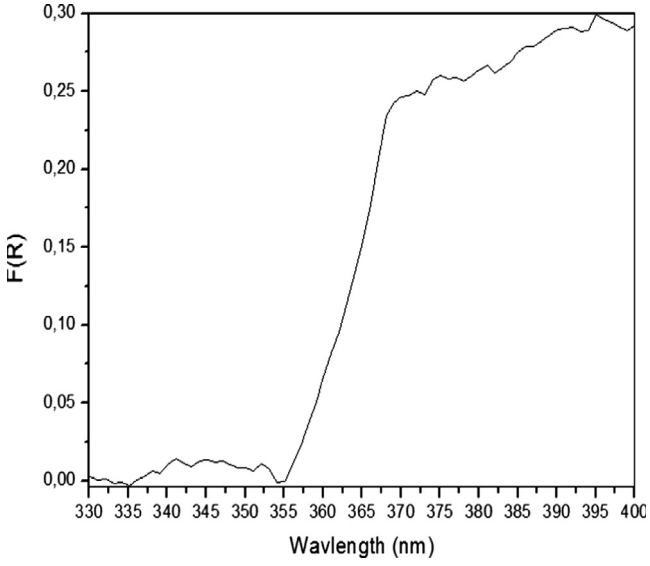

Figure 4 UV–vis diffuse-reflectance spectrum of $Fe_2F_5(H_2O)$-(Htaz)(taz)(Hdma) after application of the Kubelka–Munk transformation.

decomposition process of the whole organic moiety leading to Fe_2O_3 as residue. Taking into account that the mass spectrometry analysis is a semiquantitative method, this only step (Fig. 3) is characterized by a significantly larger quantity of CO_2 (approximately tenth amount of NH_3 (m/z 15)) and the more abundant volatile, proving the hydrogen atoms coming from the decomposition (or oxidation) of whole organic molecules.

3.3. Optical measurement

The UV–vis diffuse-reflectance spectrum of $Fe_2F_5(H_2O)$(Htaz)(taz)(Hdma) after application of the Kubelka–Munk transformation, is displayed in Fig. 4. The energy gap value of this compound has been measured, being about 3.47 eV on the corresponding λ_{abs} (357 nm). However, this new hybrid iron fluoride material present high optical absorption in the ultraviolet (UV) region (λ < 400 nm) and good transparency in the visible range. This optical gap value belongs to similar area to that of the oxyfluorometalate (Lhoste et al., 2013).

4. Conclusions

The structure of $Fe_2F_5(H_2O)$(Htaz)(taz)(Hdma), determined by X-ray diffraction, can be described by two different octahedral $FeN_4(H_2O)_2$ monomers and $Fe_3F_{10}N_6$ trimers, whose nitrogen atoms come from neutral and deprotonated amines. In this Class II hybrid, where the iron atoms are strongly linked to the triazole molecules, the $Fe_2F_5(H_2O)$(Htaz)(taz)(Hdma) layers contain mixed valence iron. [$Hdma^+$] cations are connected by hydrogen bonds to the fluorine atoms where the distances N—H···F lie in the range 2.057–2.492 Å. This structure being regarded with the notation of Cheetham et al. (2006) shows 2-D dimensionality with respect to both organic molecules connecting metal centres (O^n) and extended inorganic connectivity (I^n), therefore the notation of Cheetham is I^0O^2 (I = inorganic and O = organic). Note that the sum of the exponents gives the overall dimensionality of the structure. In spite of the exploration of the composition space diagrams containing organic cations derived from aliphatic or cyclic amines, all searches for Class I hybrids brought eighteen compounds and no compounds for Class II hybrids.

Acknowledgment

This work was supported by the minister of superior education and research of Tunisia and Spanish MINECO (MAT2013-40950R).

References

Adil, K., Ben Ali, A., Leblanc, M., Maisonneuve, V., 2006. On isoelectronic fluorides [H3*tren*]·(AlF6)·H2O, [H3*tren*]·(AlF6)·HF, [H4*tren*]·(AlF6)·(F) and the iron analogue [H4*tren*]·(FeF6)·(F). Solid State Sci. 8, 698–703.

Adil, K., Saada, M.A., Ben Ali, A., Body, M., Dang, M.T., Hémon-Ribaud, A., Leblanc, M., Maisonneuve, V., 2007. Hydrogen bonded H_3O^+, H_2O, HF, F^- in fluoride metalates (Al, Cr, Fe, Zr, Ta) templated with tren (tris-(2-aminoethyl)amine). J. Fluorine Chem. 128, 404–412.

Adil, K., Leblanc, M., Maisonneuve, V., 2009. Evidence of 13 hybrid fluoroaluminates in the composition space diagram of the $Al(OH)_3$–tren–HF–ethanol system. J. Fluorine Chem. 130, 1099–1105.

Adil, K., Leblanc, M., Maisonneuve, V., Lightfoot, P., 2010. Structural chemistry of organically-templated metal fluorides. Dalton Trans. 39, 5983–5993.

Ben Ali, A., Greneche, J.M., Leblanc, M., Maisonneuve, V., 2009. $[H3tren]^{3+}$ templated iron fluorides; synthesis, crystal structures and Mossbauer studies. Solid State Sci. 11, 1631–1638.

Bentrup, U., Massa, W., Naturforsch, Z., 1991. Die Kristallstruktur von $[(CH_3)_4]FeF_4·H_2O$ mit einem di(μ-fluoro)-verbrückten $[Fe_2F_8(H_2O)_2]_2$-anion. Z. Naturforsch. B: Chem. Sci. 46, 395–399.

Brandenburg, K., Berndt, M., 1999. DIAMOND, Version 2.1.b, Crystal Impact G.R. Bonn, Germany.

Cadiau, A., Martineau, C., Leblanc, M., Maisonneuve, V., Hémon-Ribaud, A., Taulelle, F., Adil, K., 2011. $ZnAlF_5$·[TAZ]: an Al fluorinated MOF of MIL-53(Al) topology with cationic $\{Zn(1,2,4\ triazole)\}^{2+}$ linkers. J. Mater. Chem. 21, 3949–3951.

Cheetham, A.K., Rao, C.N.R., Feller, R.K., 2006. Structural diversity and chemical trends in hybrid inorganic–organic framework materials. Chem. Commun., 4780–4795

Collins, D.J., Zhou, H.C., 2007. Hydrogen storage in metal–organic frameworks. J. Mater. Chem. 17, 3154–3160.

Dong, W., 2006. Structure and magnetic properties of a dtm-bridged two-dimensional supramolecular complex $[Fe(dtm)_2(H_2O)_2(ClO_4)_2\cdot 2(H_2O)]_n$ (dtm = 4,4-ditriazolemethane). Trans. Met. Chem. 31, 801–804.

Farrugia, L.J., 1999. WinGX suite for small-molecule single-crystal crystallography. J. Appl. Crystallogr. 32, 837–838.

Férey, G., 2007. Les nouveaux solides poreux ou les miracles des trous. L'actualité chimique 304, 3–15.

Férey, G., Millange, F., Morcrette, M., Serre, C., Doublet, M., Grenéche, J.M., Tarascon, J.M., 2007. Mixed-valence Li/Fe-based metal–organic frameworks with both reversible redox and sorption properties. Angew. Chem. 46, 3259–3263.

Frommen, C., Schroder, L., Massa, W., Pebler, J., Bentrup, U., Naturforsch, Z., 1995. Magnetic studies on the 1-D antiferromagnetic chains of $enH_2Mn(Fe)F_5$. Z. Naturforsch. B – Chem. Sci. 50, 1627–1637.

Goreshnik, E., Leblanc, M., Maisonneuve, V., 2002. From isolated polyanions to 1-D structure: synthesis and crystal structure of hybrid fluorides $\{[(C_2H_4NH_3)_3NH]^{4+}\}_2\cdot(H_3O)^+\cdot[Al_7F_{30}]^{9-}$ and $\{[(C_2H_4NH_3)_3NH]^{4+}\}_2\cdot[Al_7F_{29}]^{8-}\cdot(H_2O)_2$. Z. Anorg. Allg. Chem. 628, 162–166.

Halper, S.R., Do, L., Stork, J.R., Cohen, S.M., 2006. Topological control in heterometallic metal–organic frameworks by anion templating and metalloligand design. J. Am. Chem. Soc. 128, 15255–15268.

Herdtweck, E., Graulich, J., Babel, D., Naturforsch, Z., 1990. The chain structures o f the ternary iron(III) fluorides Rb_2FeF_5 and $(CH_3NH_3)_2FeF_5$. Z. Naturforsch. B – Chem. Sci. 45, 161–169 (in German).

Kiriasis, L., Mattes, R., 1991. Ein-und zweikernige Fluorokomplexe des Titan(III), Chrom(III) und Eisen(III) Darstellung und Struktur von $(NMe_4)(Ti(H_2O)_4F_2)TiF_6,H_2O$, $(NMe_4)_3Cr_2F_9$ und $(NMe_4)_3Fe_2F_9$. Z. Anorg. Allg. Chem. 593, 90–98.

Kubelka, P., 1948. New contributions to the optics of intensely light-scattering materials. Part I. J. Opt. Soc. Am. 38, 448–457.

Lhoste, J., Galven, C., Leblanc, M., Maisonneuve, V., Rocquefelte, X., Jobic, S., Bujoli-Doeuff, M., 2013. Crystal structure and optical properties of new 0D-hybrid hydroxyfluorotitanates. Solid State Sci. 24, 101–106.

Lin, M.J., Jouaiti, A., Kyritsakas, N., Hosseini, M.W., 2009. Molecular tectonics: modulation of size and shape of cuboid 3-D coordination networks. CrystEngComm 11, 189–191.

Liu, J.Q., Wang, Y.Y., Zhang, Y.N., Liu, P., Shi, Q.Z., Battern, R., 2009. Topological diversification in metal–organic frameworks: secondary ligand and metal effects. Eur. J. Inorg. Chem. 1, 147–154.

Mahenthirarajah, T., Li, Y., Lightfoot, P., 2009. Organic–inorganic hybrid chains and layers constructed from copper-amine cations and early transition metal (Nb, Mo) oxyfluoride anions. Dalton Trans., 3280–3285

Malinovskii, S.T., Corpceanu, E.B., Bourosh, P.N., Rija, A.P., Bologa, O.A., Gdaniec, M., Bulhac, I.N., 2008. Synthesis and structure of cobalt(III) dimethylglyoximate with $[FeF_5\cdot(H_2O)]^{2-}$ anion. Russ. J. Coord. Chem. 34, 422–426.

Pachfule, P., Dey, C., Panda, T., Vanka, K., Banerjee, R., 2010. Metal organic frameworks (F-MOFs) composed of divalent transition metals, 1,10-phenanthroline, and fluorinated carboxylic acid. Cryst. Growth Des. 10, 1351–1363.

Sanchez, C., Ribot, F., 1994. Design of hybrid organic–inorganic materials synthesized via sol–gel chemistry. New J. Chem. 18, 1007–1047.

Sheldrick, G.M., 1986. In: SHELXS86. Program for the Refinement of Crystal Structures. Univ. of Gottingen, Germany.

Sheldrick, G.M., 1997. In: SHELXL97. Program for the Refinement of Crystal Structures. Univ. of Gottingen, Germany.

Smida, M., Lhoste, J., Pimenta, V., Hémon-Ribaud, A., Jouffret, L., Leblanc, M., Dammak, M., Grenèche, J.M., Maisonneuve, V., 2013. New series of hybrid fluoroferrates synthesized with triazoles: various dimensionalities and Mössbauer studies. Dalton Trans. 42, 15748–15755.

Su, Z., Fan, J., Okamura, T., Sun, Y.W., Ueyama, N., 2010. Ligand-directed and pH-controlled assembly of chiral 3d–3d heterometallic metal–organic frameworks. Cryst. Growth Des. 10, 3515–3521.

Vargas, W.E., 2002. Inversion methods from Kubelka–Munk analysis. J. Opt. A: Pure Appl. Opt. 4, 452–456.

Xing, X.Y., Mei, X.L., Li, L.C., 2011. Iron (II) coordination polymers based on 1,4-bis(1,2,4-triazol-1-ylmethyl)benzene: structure and magnetic properties. J. Mol. Struct. 922, 89–95.

Zou, R.Q., Sakurai, H., Xu, Q., 2006. Preparation, adsorption properties, and catalytic activity of 3D porous metal–organic frameworks composed of cubic building blocks and alkali-metal ions. Angew. Chem., Int. Ed. 45, 2542–2546.